Available online at www.sciencedirect.com
SCIENCE DIRECT®
Journal of Sound and Vibration 276 (2004) 1081–1091
JOURNAL OF SOUND AND VIBRATION
www.elsevier.com/locate/jsvi

Vibrational power flow characteristics of circular plate structures with peripheral surface crack

T.Y. Li*, J.X. Liu, T. Zhang

Department of Naval Architecture and Ocean Engineering, Huazhong University of Science and Technology, Wuhan 430074, China

Received 17 June 2003; accepted 20 August 2003

Abstract

In the view of structure-borne sound, the vibrational power flow of circular plates with peripheral surface crack is investigated. The peripheral surface crack is modelled as a joint of a local spring. The local stiffness of the rotational spring is deduced by using fracture mechanics and strain energy arguments. At high frequencies, the motion of bending wave and the input power flow are researched in the case of a harmonic force loaded at its center.

1. Introduction

Under fatigue load and external pulse conditions, damages may be produced as a result of the flaws or manufacturing defects in the structures. So dangers are inherent in the life of structures. For this reason, methods for making early detection and for locating of damages have been the subject of many recent investigations.

Currently available non-destructive evaluation (NDE) methods are mostly non-model methods, either visual or localized experimental methods, such as acoustic or ultrasonic methods, magnetic field methods, radiographs, eddy-current methods and thermal field methods. Accessing these techniques is time consuming and costly. Some of them are also impractical in many cases, e.g., in service ship testing and space structure. Almost all of them require that the vicinity of the damage is known in advance and that the portion of the structure being inspected is readily accessible for human beings. Subjected to these limitations, these non-model methods can provide only local information and no indication of the structural strength at a system level.

*Corresponding author.
E-mail address: ltyz@public.wh.hb.cn (T.Y. Li).

0022-460X/$ - see front matter © 2003 Elsevier Ltd. All rights reserved.
doi:10.1016/j.jsv.2003.08.013

Shortcomings of currently available NDE methods indicate a requirement of damage inspection techniques that can give global information on the structure and they do not require direct human accessibility of the structure. This requirement has led to the development of model-based methods that examine changes in the vibration characteristics of the structure.

Most of the previous researches on vibration-related damage detection are based on modal methods. The basis for such methods is that damage produces a decrease in dynamic stiffness. This decrease in turn produces decreases in natural frequencies in an undamped simple beam. This basic premise has produced a number of results using modal analysis, i.e., frequency measurement to perform diagnostics [1]. Though modal-based method may have advantages, it possess a number of major disadvantages [2].

The results of previous efforts in damage detection provide evidence that something is gained by including the effects of geometry and hence modelling the local changes in modulus. This then raises significant questions as to the validity of using traditional modal analysis (i.e., measurements of natural frequencies, assuming a uniform model) as the foundation of a damage detection.

In recent years, the structure-borne sound analysis and control of flexible structures and cabins of marine-structures and aeronautical crafts are becoming an important topic. The use of vibrational power flow in a problem of this type is very valuable. The premise of the effort proposed here is that damage to a structure will correspond in some way to changes, though small, in the structure's mass, damping and stiffness properties and so the vibrational power flow is influenced by changes of propagating waves [3].

In view of structure-borne sound, the vibrational power flow of circular plates with peripheral surface crack is investigated. The peripheral surface crack is modelled as a joint of a local spring. At high frequencies, the motion of bending wave and the input power flow are researched in the case of a harmonic force loaded at its center.

2. Theoretical model of flexural vibration

2.1. Flexural vibration of circular plate

If a thin plate is excited by a harmonic force $F_0 e^{i\omega t}$ at point (x_0, y_0), the equation governing the flexural vibration is (for brevity, the term $e^{i\omega t}$ is ignored in all the following formulas)

$$\nabla^4 w(x,y) - k^4 w(x,y) = (F_0/D)\delta(x-x_0)\delta(y-y_0), \tag{1}$$

where $\delta(\cdot)$ is *delta* function, k is flexural wave number of thin plate, $k^4 = \omega^2\rho_s/D$, ω is angular frequency, ρ_s is the material density per unit area, $D = Et^3/[12(1-v^2)]$, E, v, and t are Young's modulus, the Poisson ratio and thickness, respectively.

For circular plates, it is convenient to use a system of polar co-ordinates. If the harmonic force is loaded at the center of the plate, $x_0 = y_0 = 0$, then $r = 0$. Considering the singularity of $\delta(\cdot)$ function at the point $r = 0$ and using ignorable co-ordinates, Eq. (1) may be written as

$$\nabla^4 w - k^4 w = (F_0/D)\delta(r)/2\pi r, \tag{2}$$

where the operator

$$\nabla^4 = \left(\frac{\mathrm{d}^2}{\mathrm{d}r^2} + \frac{1}{r}\frac{\mathrm{d}}{\mathrm{d}r}\right)^2.$$

The modal solution of Eq. (2) can be written as [4]

$$w(r) = \sum_{n=1}^{\infty} \frac{F_0}{2MA_n} \frac{\phi_n(0)\phi_n(r)}{(\omega_n^2 - \omega^2 + \mathrm{i}\zeta\omega\omega_n)}, \tag{3}$$

where M is the mass of the circular plate and ζ is the loss factor defined as twice the damping ratio. The constant A_n is defined as

$$A_n = \frac{1}{R^2}\int_0^R [\phi_n(r)]^2 r\,\mathrm{d}r. \tag{4}$$

R is the radius of the circular plate. The natural frequency ω_n is defined as

$$\omega_n^2 = (D/\rho_s)(d_n/R)^2. \tag{5}$$

d_n is the non-dimensional variable. For clamped boundary, the characteristic equation about d_n is

$$\mathrm{J}_0(d_n)\,\mathrm{I}_1(d_n) + \mathrm{J}_1(d_n)\,\mathrm{I}_0(d_n) = 0, \tag{6}$$

where J_0 and J_1 are the *Bessel* functions, and I_0 and I_1 are the modified *Bessel* functions. $\phi_n(r)$ is the nth mode shape is given for clamped case [5]:

$$\phi_n(r) = \mathrm{J}_0(d_n r/R) - b_n \mathrm{I}_0(d_n r/R), \tag{7}$$

where the constant $b_n = \mathrm{J}_0(d_n)/\mathrm{I}_0(d_n)$.

In this paper, another analytical expression of Eq. (2) is used for convenience [6]:

$$u(r) = (u_0 - B)\mathrm{J}_0(kr) + B\mathrm{I}_0(kr) - \frac{\mathrm{i}F_0}{\pi Z}[\mathrm{Y}_0(kr) + 2\mathrm{K}_0(kr)], \tag{8}$$

where $u(r) = \mathrm{i}\omega w(r)$ is the vibrational velocity of the circular plate. B is a constant and $u(0)$ is the vibrational velocity of the center of the plate, which can be determined by the boundary conditions. Y_0 and K_0 are the *Bessel* functions and the modified *Bessel* functions, respectively. Z is the force impedance of the driving point. At high frequencies ($kr \gg 1$), the input point impedances of finite plates are equal to that of infinite plates [7]. Accurate input point impedance of finite circular plate is [6]

$$Z_0 = \left(-\frac{\mathrm{i}}{Z}\right)\mathrm{ctg}(kR - \pi/4), \quad Z = 8(D\rho_s)^{1/2}. \tag{9}$$

The *Bessel* functions and the modified *Bessel* functions may be given with their asymptotic expressions [8]:

$$\begin{aligned} &\mathrm{J}_0(kr) = \sqrt{2/\pi kr}\cos(kr - \pi/4), \quad \mathrm{Y}_0(kr) = \sqrt{2\pi/kr}\sin(kr - \pi/4), \\ &\mathrm{I}_0(kr) = \mathrm{e}^{-k(R-r)}/\sqrt{2\pi kr}, \quad \mathrm{K}_0(kr) = \sqrt{\pi/2kr}\ \mathrm{e}^{-kr}. \end{aligned} \tag{10}$$

In view of expression (10), we can find that expression (8) contains cylindrical waves and nearfield waves, and the nearfield waves decay with exponential forms. At high frequencies

($kr \gg 1$), the response of the circular plate is dominated by the cylindrical waves except the domains near the center point and the boundaries of the circular plate.

For the circular plates with clamped supports, B and $u(0)$ are [6] given by

$$B = \frac{[\mathrm{i}(F_0/\pi Z)(\mathrm{Y}_0' + 2\mathrm{K}_0')] - u_0\mathrm{I}_0'}{\mathrm{I}_0' - \mathrm{J}_0'}, \tag{11}$$

$$\frac{u_0}{F_0} = \frac{\mathrm{i}}{\pi Z}\frac{(\mathrm{Y}_0' + 2\mathrm{K}_0')(\mathrm{I}_0 - \mathrm{J}_0) - (\mathrm{Y}_0 + 2\mathrm{K}_0)(\mathrm{I}_0' - \mathrm{J}_0')}{\mathrm{J}_0'\mathrm{I}_0 - \mathrm{I}_0'\mathrm{J}_0}, \tag{12}$$

where the superscript denotes differentiation with respect of the argument kr. After differentiation, the variable of the *Bessel* functions and the modified *Bessel* functions is kR.

For symmetric flexural vibration, the shear force and bending moment in the radial direction are, respectively,

$$Q_r = D\frac{\partial}{\partial r}\left(\frac{\partial^2 w}{\partial r^2} + \frac{1}{r}\frac{\partial w}{\partial r}\right), \quad M_r = -D\left(\frac{\partial^2 w}{\partial r^2} + \frac{v}{r}\frac{\partial w}{\partial r}\right). \tag{13}$$

Based on the above analysis, a state vector equation of the circular plate may be written as

$$\begin{Bmatrix} w \\ \theta \\ M \\ Q \\ 1 \end{Bmatrix} = [\nabla]\begin{Bmatrix} u_0 \\ B \\ 1 \end{Bmatrix}, \tag{14}$$

where all element expressions of the matrix $[\nabla]$ can be easily obtained by expressions (8) and (13). To deal with the load terms conveniently, the constant "1" is used in Eq. (14).

2.2. Peripheral surface crack model

At $r = r_c$, there is a peripheral surface crack which is satisfied with the conditions of linear elastic theory. In this paper, the research is only limited on the bending vibration of the circular plate, therefore, it can be considered that the crack mostly induces the discontinuity of the rotation. Then the crack can be simplified as a local peripheral rotational spring [9]. The rotational stiffness of the local spring is $K_{rc}(a)$, where a is the depth of the surface crack. The relationship between the depth and the rotation stiffness of the crack may be derived from fracture mechanics theory and strain energy method. Generally, this relationship is approximate and known results for the stress intensity of cracked rectangular beams may be used.

For the sake of convenience, define the non-dimensional rotational stiffness as

$$K = K_{rc}(a)\frac{2t}{D}, \tag{15}$$

where t is the thickness of the circular plate. In the case of flexural vibration, the rotating angle $\theta_{rc}(a)$ of a strip with a peripheral surface crack due to bending moment $M_{rc}(a)$ may be written as

$$\theta_{rc}(a) = \frac{\partial}{\partial M_{rc}(a)}\int_0^a J\,\mathrm{d}a, \tag{16}$$

where $M_{rc}(a)$ is the bending moment at $r = r_c$. The strain energy release function J, for the opening mode of fracture and a strip of width $a\,\mathrm{d}\varphi$, with a crack of depth a is

$$J = \int_0^{2\pi} \frac{K_1^2}{E}\,\mathrm{d}\varphi, \tag{17}$$

where $\mathrm{d}\varphi$ is the micro-increment of rotation between both sides of the crack strip due to flexural vibration. K_1 is the stress intensity factor, and E is Young's modulus of the circular plate. According to fracture mechanics theory, an expression can be obtained:

$$\frac{1}{K_{rc}(a)} = \frac{\partial^2}{\partial M_{rc}^2}\int_0^a J\,\mathrm{d}a. \tag{18}$$

From Eqs. (16)–(18), the local rotational stiffness $K_{rc}(a)$ may be computed by appropriate use of K_1 for the cracked strip. From Ref. [10], by suitable rearrangement of terms, integration and substitution in Eqs. (17) and (18), the non-dimensional rotational stiffness K is given by

$$K = \frac{1}{3F_1(\eta)}, \tag{19}$$

where

$$\eta = \frac{a}{2t},$$
$$F_1(\eta) = 1.862\eta^2 - 3.95\eta^3 + 16.37\eta^4 - 37.226\eta^5 + 75.81\eta^6 - 126.9\eta^7 + 172.5\eta^8 + 143.97\eta^9 + 66.56\eta^{10}.$$

The model about local rotational spring expressed by Eq. (19) can be used for crack depth up to 0.8 of the plate thickness [9].

2.3. Transfer matrix of vibrating wave propagating

Eq. (8) is an analytical expression of the ideal circular plates with fully clamped supports. When there are peripheral surface cracks on the circular plate, a transfer matrix can be used to express the propagation of the bending vibrational waves.

For brevity, the domain of $r \leqslant r_c$ is denoted by subscript "1", and the domain of $r \geqslant r_c$ is denoted by subscript "2".

When $r \geqslant r_c$, the expression of the free flexural vibration is [11]

$$w_2(r) = A_1\mathrm{J}_0(kr) + A_2\mathrm{Y}_0(kr) + A_3\mathrm{I}_0(kr) + A_4\mathrm{K}_0(kr), \tag{20}$$

where A_i $(i = 1, 2, 3, 4)$ are constants which are determined by the boundary conditions of the circular plate.

For the cross-section of the circular plate when $r \geqslant r_c$, the state vector equation is

$$\begin{Bmatrix} w_2 \\ \theta_2 \\ M_2 \\ Q_2 \\ 1 \end{Bmatrix} = [\Delta_2] \begin{Bmatrix} A_1 \\ A_2 \\ A_3 \\ A_4 \\ 1 \end{Bmatrix}, \tag{21}$$

where the elements of the matrix $[\Delta_2]$ may also derived from expressions (13) and (20). At the boundary of $r = r_c$, the state vector equation of is

$$\begin{Bmatrix} w_2 \\ \theta_2 \\ M_2 \\ Q_2 \\ 1 \end{Bmatrix}_{r_c} = [\Delta_2]_{r_c} \begin{Bmatrix} A_1 \\ A_2 \\ A_3 \\ A_4 \\ 1 \end{Bmatrix}. \tag{22}$$

From Eq. (22), constants A_i $(i = 1, 2, 3, 4)$ can be expressed as

$$\begin{Bmatrix} A_1 \\ A_2 \\ A_3 \\ A_4 \\ 1 \end{Bmatrix} = [\Delta_2]_{r_c}^{-1} \begin{Bmatrix} w_2 \\ \theta_2 \\ M_2 \\ Q_2 \\ 1 \end{Bmatrix}_{r_c}. \tag{23}$$

Substituting Eq. (23) into Eq. (21), the state vector equation of $r \geqslant r_c$ may be written as in the form of transfer matrix:

$$\begin{Bmatrix} w_2 \\ \theta_2 \\ M_2 \\ Q_2 \\ 1 \end{Bmatrix} = [\Delta_2][\Delta_2]_{r_c}^{-1} \begin{Bmatrix} w_2 \\ \theta_2 \\ M_2 \\ Q_2 \\ 1 \end{Bmatrix}_{r_c} = [\Delta] \begin{Bmatrix} w_2 \\ \theta_2 \\ M_2 \\ Q_2 \\ 1 \end{Bmatrix}_{r_c}. \tag{24}$$

At $r = r_c$, the continuity conditions are

$$\begin{aligned} w_2 &= w_1, \\ M_2 &= M_1, \\ Q_2 &= Q_1. \end{aligned} \tag{25}$$

Because rotational springs exist at $r = r_c$, the compatible conditions are

$$w_2' = w_1' + \frac{M_{r_c}}{K_{r_c}}. \tag{26}$$

According to expression (13), expression (26) can be transferred to another form:

$$w_2' = w_1' - \frac{\lambda}{K} w_1'' - \frac{v\xi}{K} w_1', \tag{27}$$

where λ is the non-dimensional frequency, $\lambda^4 = (2tK)^4 = (16\omega^2\rho_s t^4)/D$, $\xi = 2t/r_c$.

Applying the form of point transfer matrix, expressions (25) and (27) can be written as follows:

$$\begin{Bmatrix} w_2 \\ \theta_2 \\ M_2 \\ Q_2 \\ 1 \end{Bmatrix}_{r_c} = [C] \begin{Bmatrix} w_1 \\ \theta_1 \\ M_1 \\ Q_1 \\ 1 \end{Bmatrix}_{r_c}, \tag{28}$$

where $[C]$ is point transfer matrix. According to coupling conditions of peripheral surface cracks that are expressed by Eqs. (14), (24) and (28), a transfer matrix equation can be obtained:

$$\begin{Bmatrix} w_2 \\ \theta_2 \\ M_2 \\ Q_2 \\ 1 \end{Bmatrix} = [\Delta][C][\nabla] \begin{Bmatrix} u_0 \\ B \\ 1 \end{Bmatrix} = [\beta] \begin{Bmatrix} u_0 \\ B \\ 1 \end{Bmatrix}, \tag{29}$$

where $[\beta] = [\Delta][C][\nabla]$.

At high frequencies, when the radius and the damping of the structure are rather large, the proportion of the nearfield waves is very small in the solution of flexural vibration and its influence can be ignored and expression (8) can be simplified in the region of $r < r_c$ [6]:

$$u(r) = (u_0 - B)\mathrm{J}_0(kr) - \frac{\mathrm{i}F_0}{\pi Z}\mathrm{Y}_0(kr). \tag{30}$$

This simplification not only avoids complex calculations but insures enough precision.

To the circular plate structure, its boundary ($r = R$) is clamped, and hence the boundary conditions are:

$$\begin{aligned} w_2 &= 0, \\ \theta_2 &= 0. \end{aligned} \tag{31}$$

Substitution of expression (31) into expression (29) results in following equations:

$$\begin{aligned} \beta_{11}(R)u_0 + \beta_{12}(R)B + \beta_{13}(R) &= 0, \\ \beta_{21}(R)u_0 + \beta_{22}(R)B + \beta_{23}(R) &= 0. \end{aligned} \tag{32}$$

The unknown argument u_0 and B could be solved by the above equations, and then the problem of the bending waves of the whole system can be computed.

2.4. Vibrational power flow analysis

As above analysis, when the damping of structures is large, only the propagating waves are considered here. Introducing complex Young's modulus $E' = E(1 + i\zeta)$, ζ is the loss factor of material, and then the complex wave number is $k(1 - i\zeta/4)$. When the response of the structure is in the state of fully stability, the vibrating energy input by the excitation is continuously exhausted by the damping. The input power flow by the point load to the circular plate is [12] given by

$$P_s = \tfrac{1}{2}\mathrm{Re}(F_0 u_0^{\otimes}), \tag{33}$$

where $\otimes$ denotes complex conjugations.

For perfect circular plate, The input power flow at high frequency can be written as

$$P_s = \tfrac{1}{2}|F_0|^2 \mathrm{Re}(1/Z^{\otimes}) \tag{34}$$

According to the statistical energy analysis (SEA), $Z = 8(D\rho_s)^{1/2}$ is constant. So input power flow is also a constant at high frequency.

The input power flows of the perfect circular plate and the cracked circular plate could be obtained by Eq. (33). In practical measurement, the value of the input power flow can be measured with the impedance head [13].

3. Results and discussions

In this paper, the parameters are chosen such that $R = 1.0\,\mathrm{m}$, $t = 0.01\,\mathrm{m}$, $v = 0.3$, $\eta = a/2t = 0.8$, $r_c = 0.5R$, $E = 2.0 \times 10^{11}\,\mathrm{N/m^2}$. Fig. 1 shows the input power flows of the perfect circular plate and the cracked circular plate for different driving frequencies and loss factors. The co-ordinate of X-axis is f (Hz), and the co-ordinate of Y-axis is $\log_{10}(P_s/F_0^2)$ (dB). It can be seen from Fig. 1 that the analytical results and the SEA results are in good agreement with the perfect plate at high frequencies. The input power flow of the cracked plate is more than that of the perfect plate at high frequencies. Obviously, the input power flow increases with the increasing of

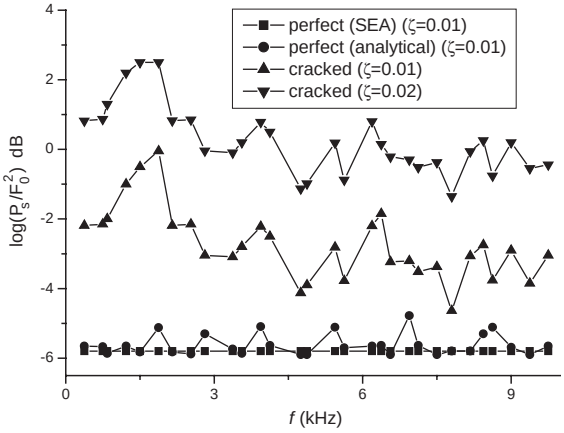

Fig. 1. The input power flow of perfect and cracked circular plates.

the loss factor of material in both cracked plate and perfect plate cases. Because the influence of loss factor is little on the natural frequencies, the curve shapes of the input power flows are almost the same for the cracked plate or for the perfect plate.

The peripheral surface crack is modelled as rotational spring in this paper. The rotational spring divides the circular plate structure into two smaller parts: the circular plate structure ($r < r_c$) and the circular ring plate structure ($r > r_c$). At higher frequencies, their vibrational modal are denser and modal density is larger than that of the perfect circular plate. Moreover, the resonant response of the structure dominates the flexural vibration. Hence when there are peripheral surface cracks in the circular plate, the damping of the circular plate structure exhausts more energy which is provide by the exterior exciting force.

Changing the parameter a/t (that implies changing the parameter η) and keeping the other parameters constant, the curves of input power flows of perfect circular plate and cracked circular plate are plotted in Fig. 2. For perfect plate, $\eta = 0$, the value of the input power flow curve is a fixed constant and the corresponding curve is a straight line. But for cracked plate, the value of the input power flow varies with the parameter a/t and the driving frequency, and at point $a/t = 0.5$, the curves have wave troughs. The value 0.5 is just the ratio of the radius and the distance between the plate center and the peripheral surface crack ($r_c/R = 0.5$). Meantime, Fig. 2 shows that the driving frequency has an effect on the input power flow of cracked plate.

Fig. 3 shows the curves of the input power flows of the perfect circular plate and the cracked circular plate when changing the parameter r_c/R and fixing the other parameters. For cracked plate, the value of input power flow varies with the parameter r_c/R and the driving frequency. At $r_c/R = 0.8$, curves have peaks. The value 0.8 is just the ratio of the thickness of the circular plate and the depth of the peripheral surface crack ($\eta = a/2t = 0.8$). Meantime, Fig. 2 shows that the driving frequency has an effect on the input power flow of cracked plate.

At high frequencies, the results have enough precision. But at low frequencies, the results have little accuracy because of the application of impedance expression of high frequencies and the omission of nearfield waves.

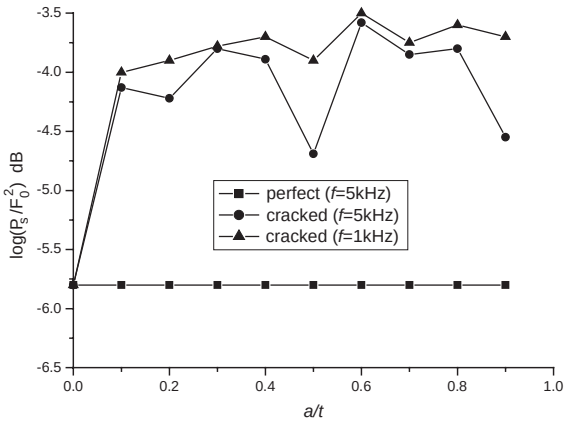

Fig. 2. The input power flow when changing a/t ($\zeta = 0.01$).

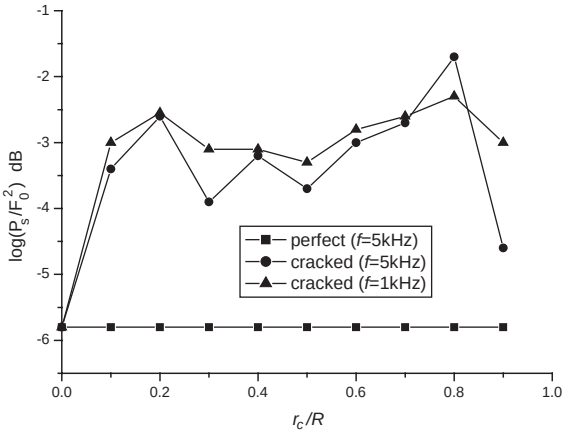

Fig. 3. The input power flow when changing $r_c/R\,(\zeta = 0.01)$.

4. Conclusion

This paper presented an approach to analyze vibrational power flow characteristics of circular plate structures with peripheral surface crack. When there is peripheral surface crack in the circular plate, the peripheral surface crack is modelled as a joint of a local rotational spring. The local stiffness of the rotational spring is deduced by the fracture mechanic theories. At high frequencies, the motion of bending wave and the input power flow are researched.

This paper assumed a harmonic transverse force loading at the center of circular plate and non-modal solution is used for convenience, so point transfer matrix can be easily applied. If the types of forces and position have been changed, the transverse vibrational expression of circular plate has to make use of the form of modal solution. In this case, detailed procedure will be given in a planned future work.

Further work will be done to diagnose the crack based on the power flow analysis presented in this paper.

References

[1] T.C. Tsai, Y.Z. Wang, Vibration analysis and diagnosis of a cracked shaft, *Journal of Sound and Vibration* 192 (1996) 607–620.
[2] H.T. Banks, D.J. Inman, D.J. Leo, et al., An experimentally validated damage detection theory in smart structures, *Journal of Sound and Vibration* 191 (1996) 859–880.
[3] T.Y. Li, W.H. Zhang, T.G. Liu, Vibrational power flow analysis of damaged beam structures, *Journal of Sound and Vibration* 242 (2001) 59–68.
[4] H.S. Kim, H.J. Kang, J.S. Kim, A vibration analysis of plates at high frequencies by the power flow method, *Journal of Sound and Vibration* 174 (1994) 404–493.
[5] R.D. Blevins, *Formalas for Natural Frequency and Mode Shape*, Van Nostrand, New York, 1979 (Chapter 11).
[6] E.J. Skudrzyk, B.R. Kautz, D.C. Greene, Vibration of, and bending-wave propagation in plates, *Journal of the Acoustical Society of America* 33 (1961) 36–45.
[7] L. Cremer, M. Heckl, *Structure-Borne Sound*, Springer, New York, 1973.
[8] S.Y. Liu, S.D. Liu, *Special Function*, Meteorology Press, Beijing, 1988 (in Chinese).

[9] N.K. Anifantis, R.L. Actis, A.D. Dimarogonas, Vibration of cracked annular plates, *Engineering Fracture Mechanics* 49 (1994) 371–379.
[10] N. Papaeconomou, A.D. Dimarogonas, Vibration of cracked beams, *Computer Mechanics* 5 (1989) 88–94.
[11] Z.L. Xu, *Theory of Elasticity*, Higher Education Press, Beijing, 1990 (in Chinese).
[12] T.Y. Li, X.M. Zhang, Y.T. Zuo, et al., Structural power flow analysis for a floating raft isolation system consisting of constrained damped beams, *Journal of Sound and Vibration* 202 (1997) 47–54.
[13] T.Y. Li, L. Liu, T.G. Liu, Energy flow analysis method of identification of structure-borne sound source, *Chinese Journal of Mechanical Engineering* 35 (1999) 29–33 (in Chinese).